Supporting Information

An interprotein Co-S coordination complex in the B_{12}-trafficking pathway

Zhu Li[1], Romila Mascarenhas[1], Umar T. Twahir[2], Albert Kallon[1], Aniruddha Deb[3], Madeline Yaw[1], James Penner-Hahn[3,4], Markos Koutmos[3,4], Kurt Warncke[2], and Ruma Banerjee[1*]

[1]Department of Biological Chemistry, University of Michigan Medical Center, Ann Arbor, MI 48109-0600; [2]Department of Physics, Emory University, Atlanta, GA 30322-2430; [3,4]Departments of Chemistry and Biophysics, University of Michigan, Ann Arbor, MI 48109

*Address correspondence to: Ruma Banerjee, 4220C MSRB III, 1150 W. Medical Center Dr., University of Michigan Medical Center, Ann Arbor, MI 48109-0600, Tel: (734) 615-5238; E-mail: rbanerje@umich.edu

Table of contents:

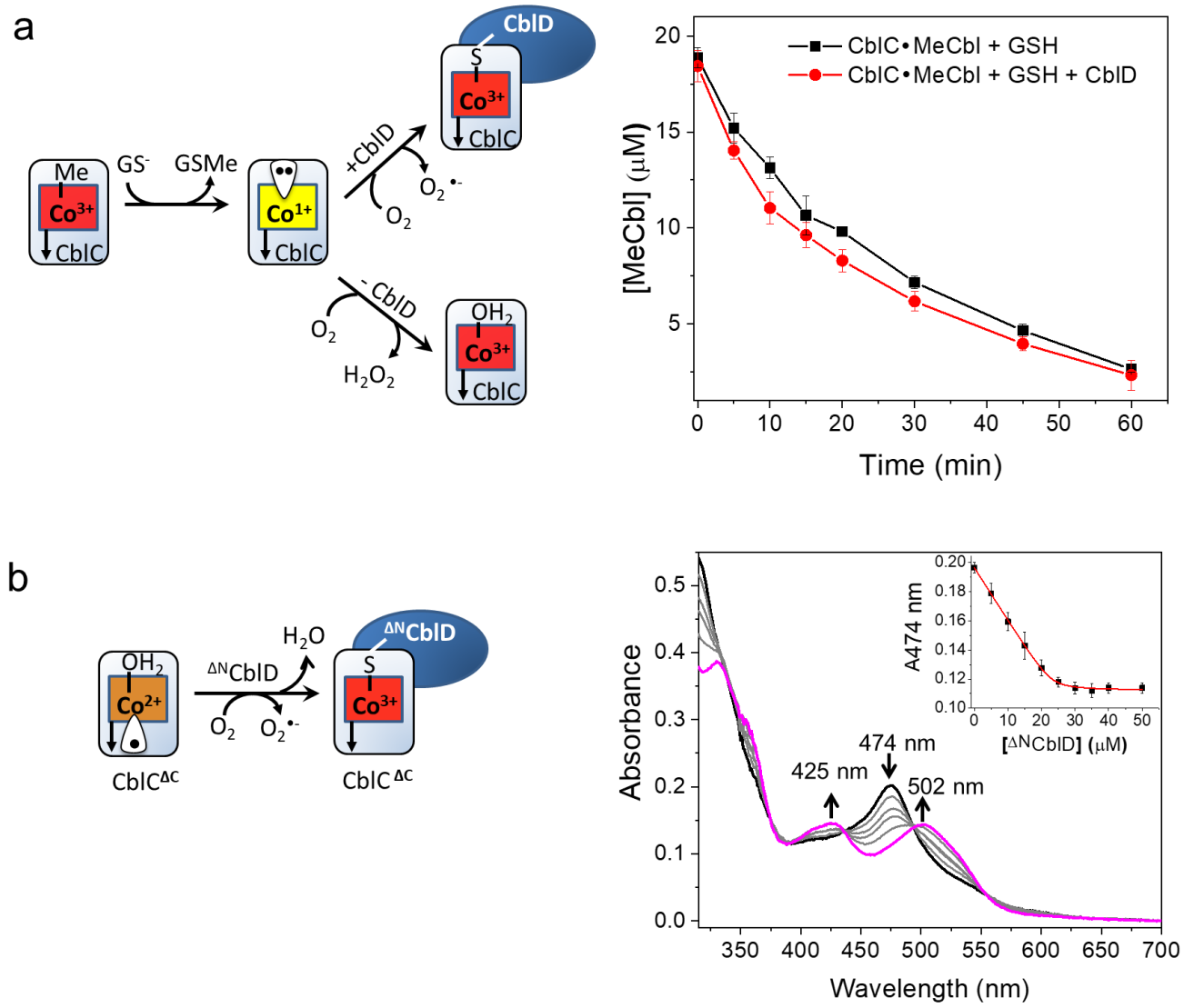

Figure S1. Characterization of CblC-catalyzed dealkylation and complex formation with truncated proteins under aerobic conditions. (a) CblD does not affect MeCbl dealkylation kinetics by CblC. The concentrations of CblC, CblD, MeCbl and GSH were 40 μM, 40 μM, 20 μM and 1 mM, respectively. The reactions were carried out at 20 °C for 1 h. The k_{obs} for dealkylation was 0.038±0.004 min^{-1} (-CblD) and 0.048±0.004 min^{-1} (+CblD). (b) Truncated variants of CblC and CblD form a thiolato-complex. Changes in the absorption spectrum of $CblC^{\Delta C}$ (40 μM)-bound cob(II)alamin (25 μM) were seen upon mixing with $^{\Delta N}$CblD (0-50 μM) under aerobic conditions. SOD (>500 U) was added to the samples to prevent $O_2^{\bullet-}$ accumulation. *Black trace*, $CblC^{\Delta C}$•cob(II)alamin; *magenta trace*, $CblC^{\Delta C}$•cob(II)alamin + $^{\Delta N}$CblD (30 μM); *gray traces* represent intermediate CblD concentration with isosbestic points of 436 and 494 nm. The *inset* shows the dependence of the change in absorbance at 474 nm on $^{\Delta N}$CblD concentration.

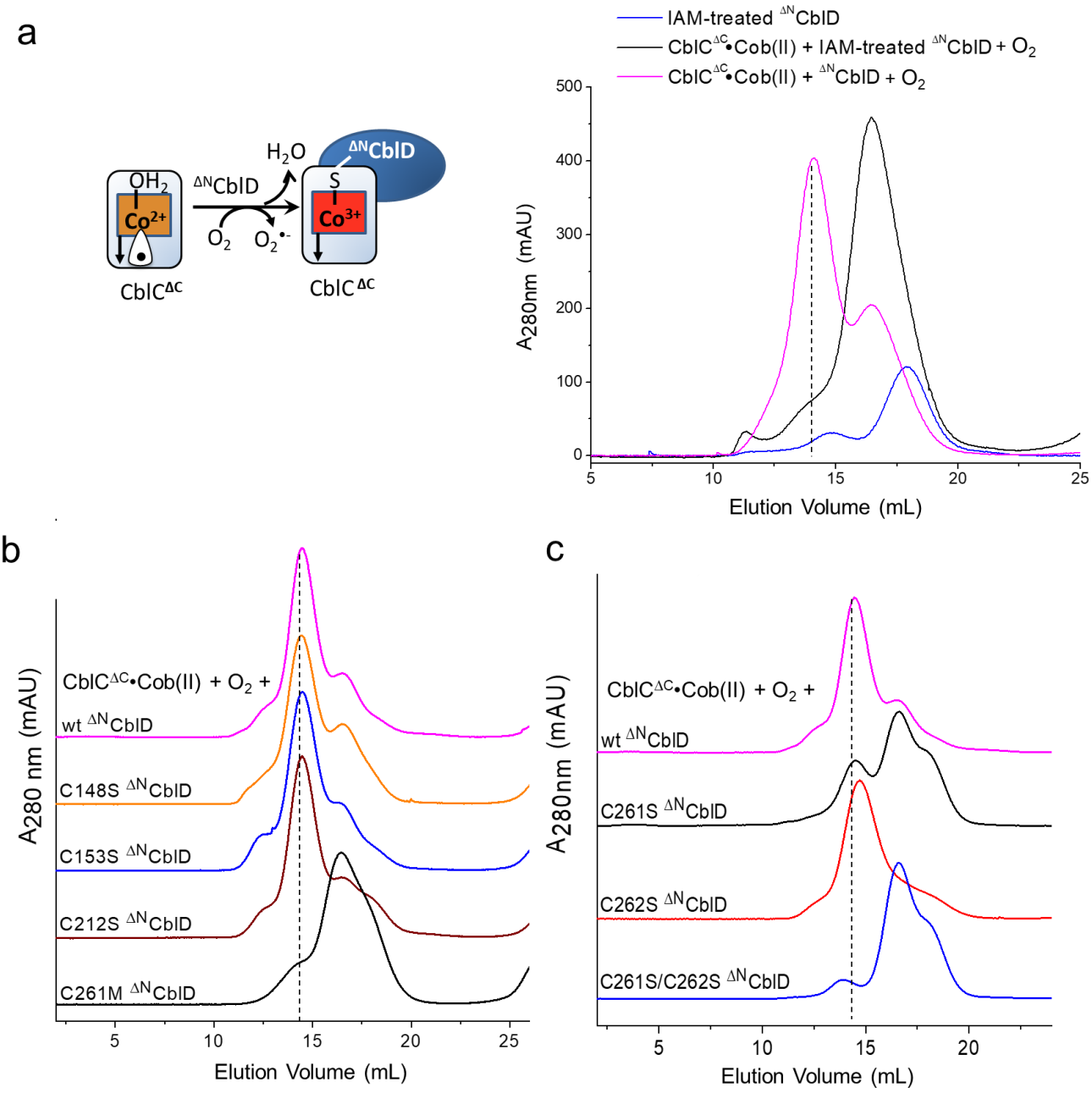

Figure S2. Identification of the cysteine ligand in the CblD•CblC complex. (a) Iodoacetamide treatment of $^{\Delta N}$CblD precludes complex formation with CblC$^{\Delta C}$. The samples as labeled in the figure, were analyzed by size exclusion chromatography. The following concentrations of reagents were used for sample preparation: CblC$^{\Delta C}$ (80 µM), cob(II)alamin (120 µM). $^{\Delta N}$CblD (80 µM) was treated with 10 mM iodoacetamide (IAM) at room temperature in the dark for 1 h. Iodoacetamide treatment induced some aggregation of $^{\Delta N}$CblD (*blue trace*). (b, c) Cys-261 provides the sulfur ligand in the CblD•CblC complex. Complex formation between CblC$^{\Delta C}$•cob(II)alamin and $^{\Delta N}$CblD was visualized by size exclusion chromatography. The samples (aerobic) as labeled in the figure, contained the following reagents: CblC$^{\Delta C}$ (80 µM), cob(II)alamin (120 µM), wild-type or mutant $^{\Delta N}$CblD (80 µM). The position of the $^{\Delta N}$CblD•CblC$^{\Delta C}$ complex is indicated by dashed lines. All samples were prepared aerobically.

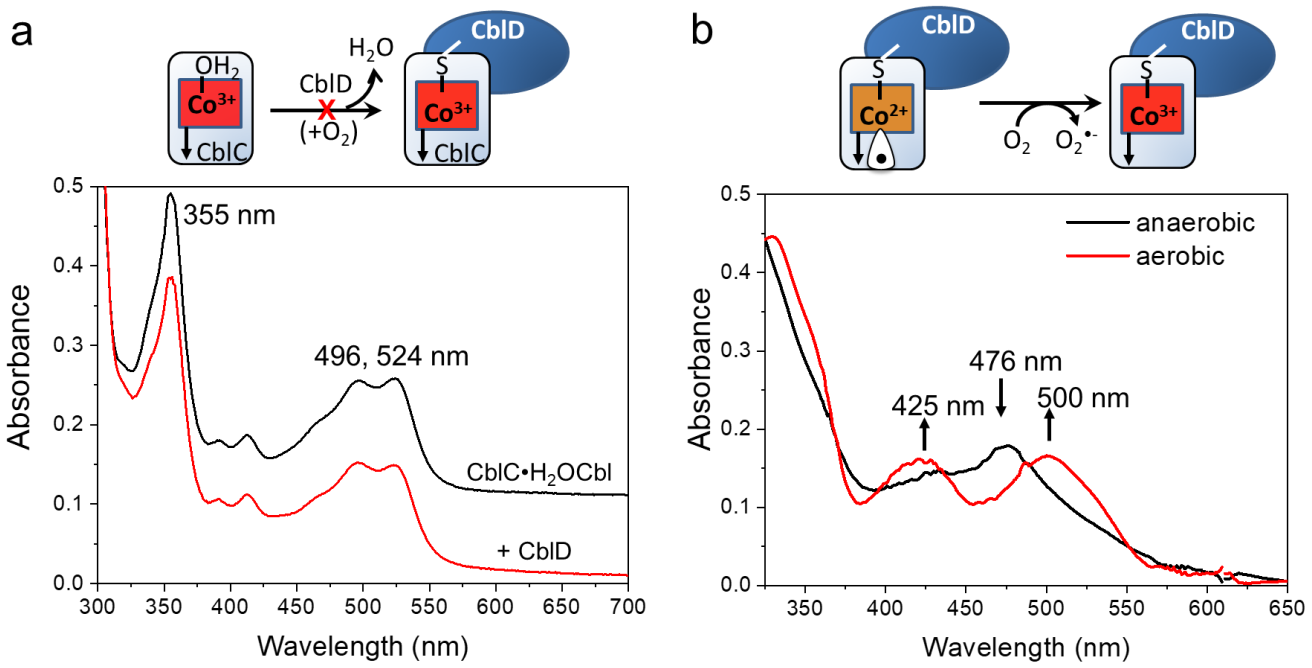

Figure S3. Cob(II)alamin bound to CblC is required for CblD•CblC complex formation. (a) Thiolato-cob(III)alamin is not formed upon mixing CblD with CblC•H_2OCbl. The samples as labeled contained: CblC (40 μM)•H_2OCbl (20 μM), which was prepared by incubating CblC (40 μM)•MeCbl (20 μM) with 1 mM GSH aerobically at room temperature for 1 h, followed by removal of GSH by extensive washing in an Amicon filtration unit. Addition of CblD (40 μM) did not result in spectral changes even after 1 h at room temperature under aerobic conditions. (b) Oxidation of CblC$^{\Delta C}$•cob(II)alamin in air in the presence of $^{\Delta N}$CblD. The spectrum of CblC$^{\Delta C}$ (40 μM)•cob(II)alamin (20 μM) incubated with $^{\Delta N}$CblD (40 μM) for 10 min under anaerobic conditions (*black*) changed within 2 min after introduction of air (*red*).

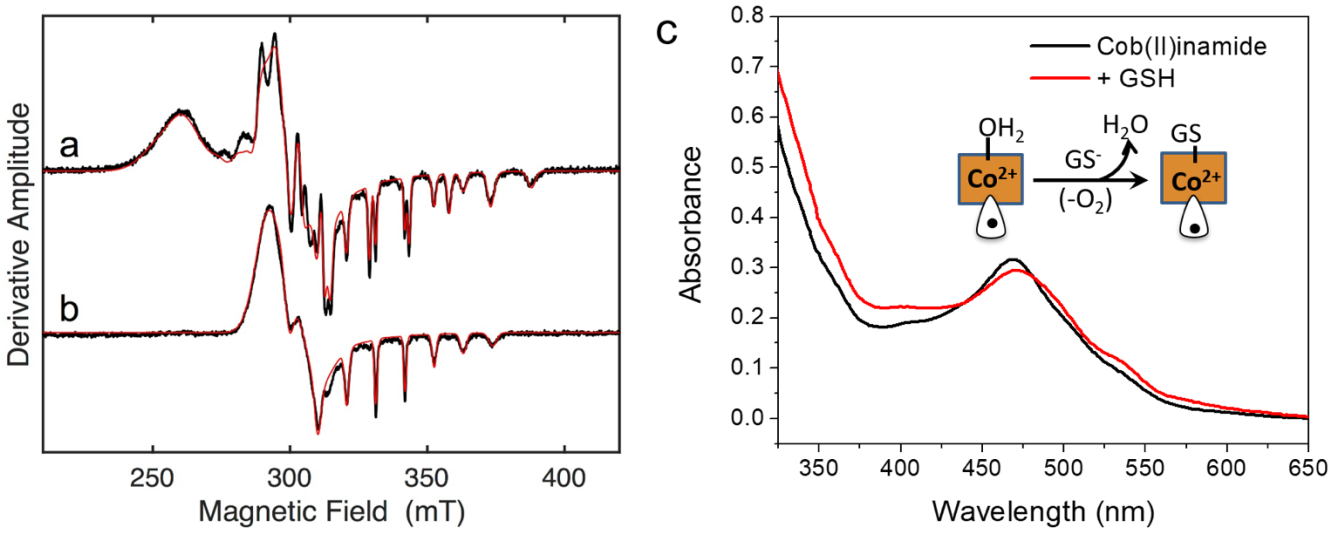

Figure S4. (a, b) Simulations of EPR spectra of thiolato-cob(II)amide species. (a) EPR spectrum of CblC$^{\Delta C}$•cob(II)alamin in the presence of $^{\Delta N}$CblD and overlaid EPR simulation (*red*). The EPR spectrum arises from two dominant components, which are assigned to DMB base-off, aquo-cob(II)alamin bound to CblC$^{\Delta C}$, and to thiolato-cob(II)alamin in the $^{\Delta N}$CblD•CblC$^{\Delta C}$ complex. The EPR simulation is a composite of these two dominant species in the normalized proportion, 0.64:0.36 (simulation parameters, Table S1). (b) EPR spectrum of cob(II)inamide in the presence of 4 mM GSH (GS^- form, basic pH) and overlaid EPR simulation (*red*). The single-component EPR spectrum is assigned to thiolato-cob(II)alamin. The amplitude is scaled to match the amplitude of the thiolato-cob(II)alamin component in (a). Identical simulation parameters for the thiolato-cob(II)alamin are used for the spectra in (a) and (b) (Table S1). Free electron *g*=2.002 corresponds to 337.1 mT. (c) Comparison of the UV-visible spectra of cob(II)inamide (*black*) and GS^--cob(II)inamde (*red*) under anaerobic conditions. The samples were prepared in 0.2 M NaOH + 10 % glycerol (v/v). The concentrations of cob(II)inamide and GSH were 30 µM and 6 mM respectively. The λ_{max} values are 469 (-GSH) and 472 nm (+ GSH), respectively.

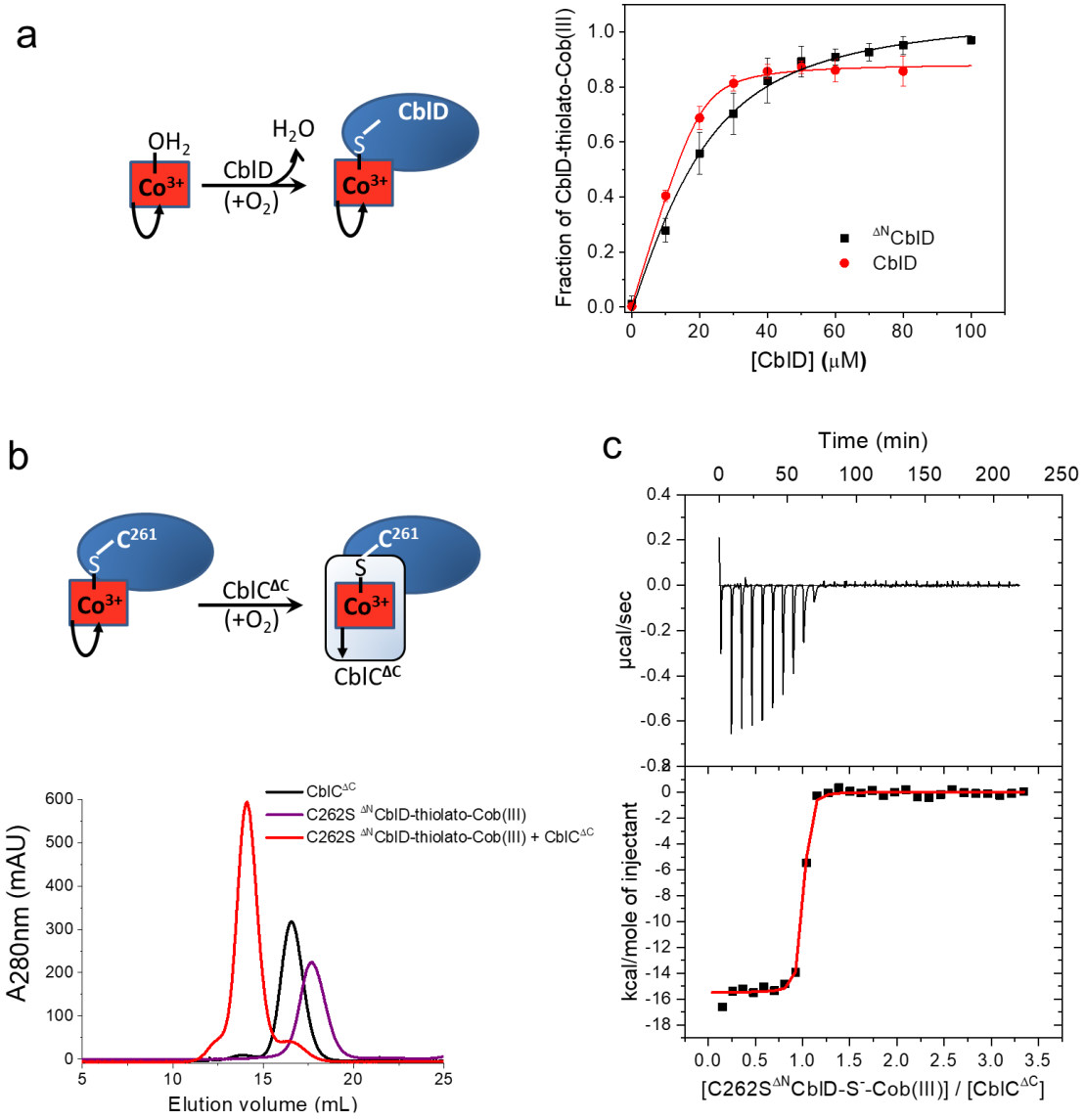

Figure S5. Characterization of H_2OCbl coordination to CblD under aerobic conditions. (a) Titration of H_2OCbl binding to wild-type CblD (*red*) or $^{\Delta N}$CblD (*black*). H_2OCbl (20 μM) was incubated with 0-100 μM CblD at room temperature for 1 h. The fraction of B_{12} in the thiolato-form was quantified based on the absorbance at 351 nm. The estimated K_D values are 1.0 ± 0.4 μM and 9.1 ± 1.6 μM for CblD and $^{\Delta N}$CblD, respectively and represent the mean ± SD of 3 independent measurements. (b) Complex formation between C262S $^{\Delta N}$CblD-thiolato-cob(III)alamin and CblC$^{\Delta C}$. Size exclusion chromatography analysis of the samples as labeled containing: CblC$^{\Delta C}$ (66 μM), C262S $^{\Delta N}$CblD (60 μM) + H_2OCbl (300 μM). C262S $^{\Delta N}$CblD and H_2OCbl were incubated at room temperature in the dark for 1 h followed by removal of excess H_2OCbl prior to addition of CblC$^{\Delta C}$ on ice for 10 min. (c) ITC titration of C262S $^{\Delta N}$CblD-thiolato-cob(III)alamin binding to CblC$^{\Delta C}$. CblC$^{\Delta C}$ (10 μM) was titrated at 20 °C with 29 × 10 μl injections of C262S $^{\Delta N}$CblD-thiolato-cob(III)alamin (120 μM). The data are representative of 4 independent experiments. The data were fit to a one-site model and yielded the following values: K_D = 0.04 ± 0.02 μM, N = 1.00 ± 0.08, ΔH = -14 ± 2 kcal/mol, and TΔS = -4 ± 2 kcal/mol (mean ± SD, n=4).

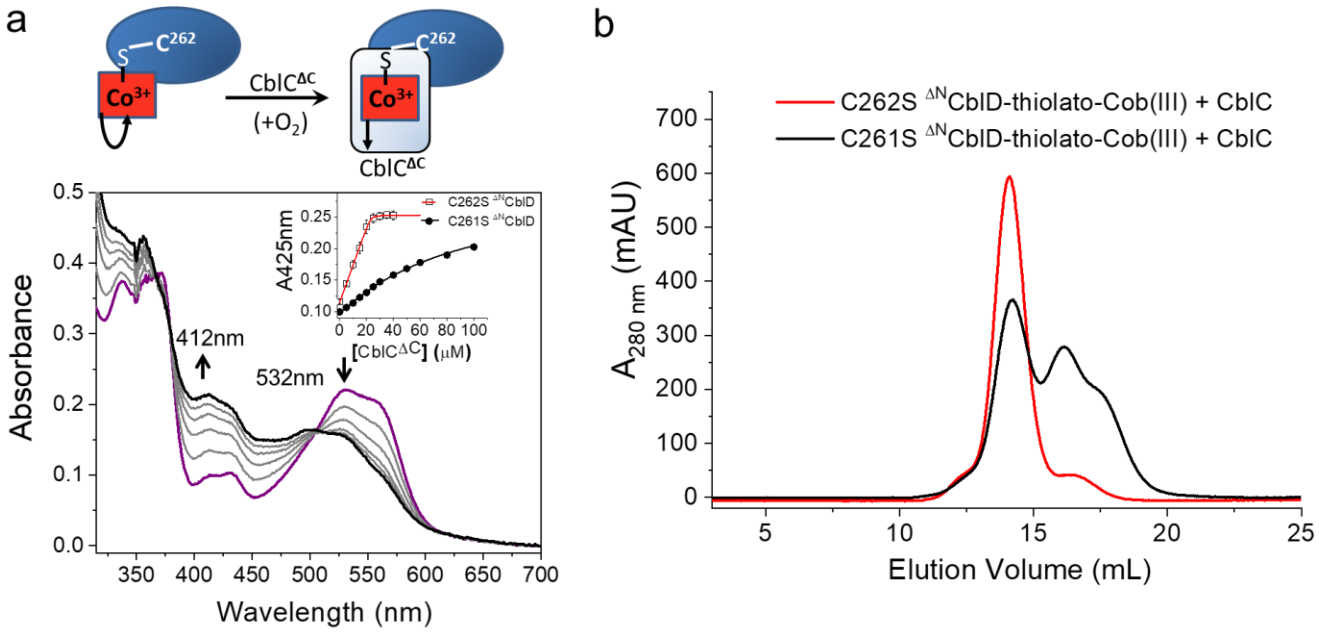

Figure S6. Complex formation between C261S $^{\Delta N}$CblD-thiolato-cob(III)alamin and CblC$^{\Delta C}$ under aerobic conditions. (a) Changes in the absorption spectrum of thiolato-cob(III)alamin bound to C261S $^{\Delta N}$CblD (25 μM) upon mixing with CblC$^{\Delta C}$ (0-100 μM). The initial and final spectra are in purple and black, respectively. *Inset*. Dependence of A425 nm on the concentration of CblC$^{\Delta C}$. (b) Complex formation between $^{\Delta N}$CblD-thiolato-cob(III)alamin variants and CblC$^{\Delta C}$ as monitored by size exclusion chromatography. The samples contained CblC$^{\Delta C}$ (60 μM) and $^{\Delta N}$CblD-thiolato-cob(III)alamin (60 μM) generated with the C261S or C262S variant. The efficiency of complex formation was lower with the C261S mutant of $^{\Delta N}$CblD.

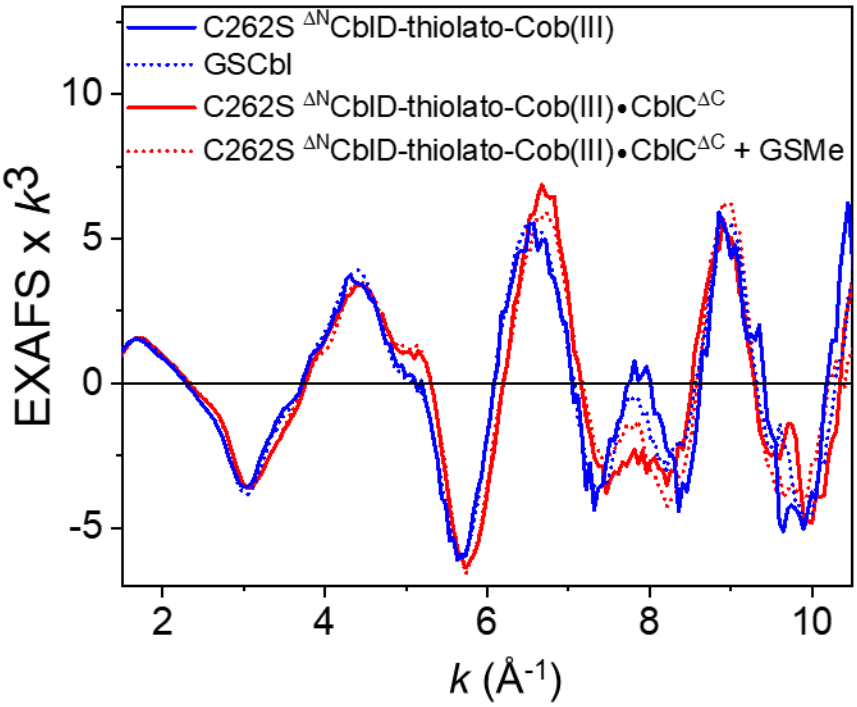

Figure S7. Comparison of base-on (*blue*) and base-off (*red*) EXAFS spectra. k^3 weighted EXAFS amplitude for all four samples are compared. Although the spectra are generally similar, consistent with the presence of a cobalamin ligand in all four cases, there are small differences, particularly in the k=6-8 Å^{-1} region, between the base on samples (C262S $^{\Delta N}$CblD-thiolato-cob(III)alamin and GSCbl, in blue) and the base-off samples (C262S $^{\Delta N}$CblD-thiolato-cob(III)alamin•CblD$^{\Delta C}$ with or without added GSMe, in red).

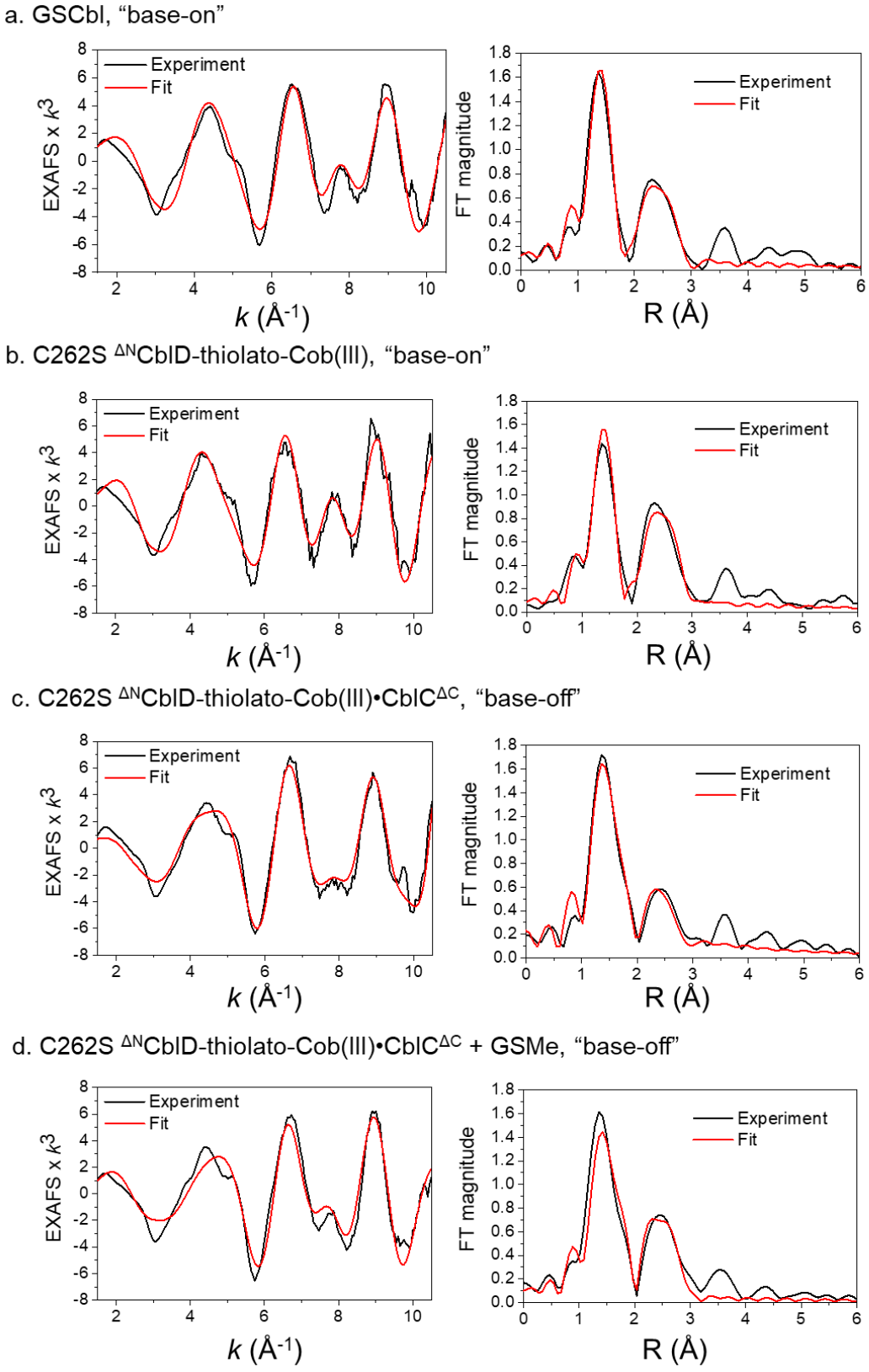

Figure S8. Experimental and fitted EXAFS data for Co-S containing cobamides. *Left*. k^3 weighted EXAFS. *Right*. Magnitude of the Fourier transform of the k^3 weighted EXAFS.

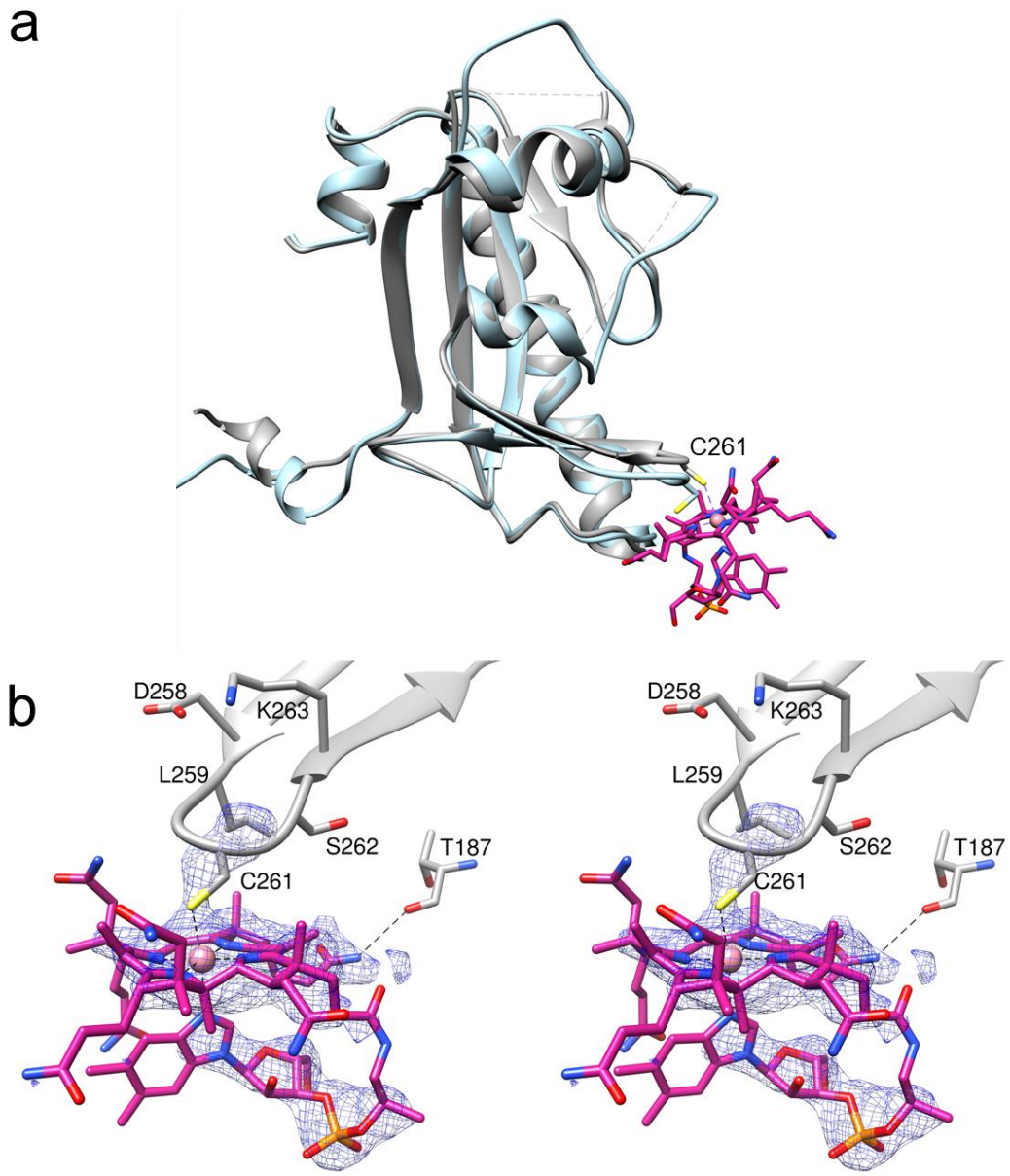

Figure S9. (a) Overlay of the structures of $^{\Delta N}$CblD with and without cobalamin. The structures of $^{\Delta N108}$CblD (*blue*) (PDB code: 5CV0) and C262S $^{\Delta N}$CblD thiolato-cob(III)alamin (*grey*) (RMSD= 0.63 Å) shows that cobalt coordination did not induce a major conformational change in the protein. (b) Stereo view of a close-up showing the interactions between cobalamin and CblD with superimposition of the Fo-Fc simulated annealing omit map of cobalamin and Cys-261 at 2.5 σ.

Table S1: EPR simulation parameters for spectra of the $^{\Delta N}$CblD•CblC$^{\Delta C}$ complex and thiolato-cob(II)inamide.[a]

Sample	Component	g_x	g_y	g_z	A_x (^{59}Co) (MHz)	A_y (^{59}Co) (MHz)	A_z (^{59}Co) (MHz)
$^{\Delta N}$CblD•CblC$^{\Delta C}$ [b]	1	2.459	2.340	1.999	235	235	405
	2	2.234	2.234	2.007	49.2	49.2	300
thiolato-cob(II)inamide [c,d]	-	2.234	2.234	2.007	49.2	49.2	300

[a]The simulation parameters correspond to the EPR spectra in Figure S4a. The g_x, g_y, and g_z correspond to principal values of the electron g tensor, in descending order. The principal values of the hyperfine (A) tensor, A_x, A_y, and A_z, correspond to interaction of the unpaired electron (spin, S=1/2) with the ^{59}Co nucleus (spin, I=$^7/_2$). The principal axes of the g and A tensors are colinear. The hyperfine splitting characterized by A_z is clearly resolved in the spectra at high magnetic field [narrow trough features arrayed symmetrically about the g_z position; a_z (component 1) = 14.5 mT; a_z (component 2) = 10.7 mT. Superhyperfine coupling from interactions of the unpaired electron spin with the directly coordinated axial ligand nucleus is not detected, owing to the low natural abundance of the I>0 nuclei of O (0.04%) and S (0.8%).

[b] The simulation is the sum of two components, which are assigned to DMB base-off, aquo-cob(II)alamin bound to CblC$^{\Delta C}$ (1; normalized proportion, 0.64), and to thiolato-cob(II)alamin in the $^{\Delta N}$CblD•CblC$^{\Delta C}$ complex (2; 0.36).

[c] The thiolato-cob(II)inamide model complex has axial g tensor symmetry (g_x=g_y>g_z), relative to the rhombic symmetry in the DMB base-off/aquo base-on cob(II)alamin component (g_x>g_y>g_z). The parameters for the thiolato-cob(II)inamide complex provide an excellent simulation for the thiolato-cob(II)alamin component in the $^{\Delta N}$CblD•CblC$^{\Delta C}$ complex, and were therefore used for simulation of the composite EPR spectrum.

[d] EPR spectroscopy of thiolato-cob(II)alamin (pH≤1) and thiolato-cob(II)inamide (pH=4 and 8-10) complexes has been reported[1]. Comparable g (g_x=g_y=2.275, g_z=2.001) and A (A_x=A_y=69 MHz, A_z=279 MHz) tensor principal values were measured for the 2-ethanethiolato-cob(II)inamide complex under basic pH conditions, which correspond to the alkaline conditions for the sample of cob(II)inamide mixed with glutathione.

Table S2. Summary of Co EXAFS simulations.[a]

Sample/model	Co-S		Co-N[d]		Co···C[e]	
	R (Å)[b]	σ^2 (Å^2)x10^3 [c]	R (Å)[b]	σ^2 (Å^2)x10^3 [c]	R (Å) [e]	σ^2 (Å^2) x10^3 [c]
GSCbl (base-on thiolato-cob(III)alamin)	2.23	2.2	1.87/1.90	2.4	2.93	2.9
C262S $^{\Delta N}$CblD (base-on thiolato-cob(III)alamin)	2.24	2.6	1.88/1.91	3.3	2.92	2.1
C262S $^{\Delta N}$CblD•CblC$^{\Delta C}$ (base-off thiolato-cob(III)alamin)	2.57	6.9	1.87/1.90	2.8	2.91	6.3
C262S $^{\Delta N}$CblD•CblC$^{\Delta C}$ + GSMe (base-off thiolato-cob(III)alamin)	2.56	3.4	1.86/1.89	2.9	2.92	3.3

[a]The seven refined parameters giving the best fits. In addition to the refined parameters, FEFF scattering pathways were included for all major paths out to 3.4 Å with distances linked to the refined Co–nearest-neighbor distance. Coordination numbers were fixed at 1 (Co-S), 4 or 5 for the Co-N shell (see below) with path degeneracies of 8, 16, 8, and 3 for the Co-N-C paths at ~2.9, 3.1, 3.30, and 3.33 Å respectively, based on the known cobalamin structure. Debye-Waller factors for all of the outer shells were taken from values calculated by Dimakis and Bunker [2] and were linked geometrically to the refined nearest-neighbor values.

[b]Fitted Co–nearest-neighbor distance.

[c]Fitted RMS deviation in distance (Debye-Waller factor).

[d]Corrins are known to have significant variation in the Co-N distances. Because there were not sufficient independent data points to justify more than one Co-N distance, a series of fits were attempted with $R_{Co\text{-}N}$ fixed at 2 different distances, with only the *average* Co-N distance refined in order to explore whether distortion in the Co-N distances might account for the observed variation in the EXAFS at k~8 Å^{-1}. These fits were only slightly better than fits using a single Co-N shell and could not account for the variation at k~8 Å^{-1}. Therefore, for all of the fits reported here, $\Delta R_{Co\text{-}N}$ was fixed at 0.03 Å. Both distances are reported, however only the average $R_{Co\text{-}N}$ was refined. In order to account for the scattering from the axial base (e.g., water or DMB), fits were performed with Co-N coordination numbers of 2+2 or 2+3. There was a no significant change in either fit quality and $R_{Co\text{-}N}$, and a small increase in Debye-Waller factor.

[e]Fitted Co–next-nearest-neighbor Co-C distance. This was included as a variable parameter to account for possible ruffling of the corrin. In no case did the refined Co···C distance change by > 0.03 Å.

Table S3. Data collection and refinement statistics

C262S $^{\Delta N}$CblD-thiolato-Cob(III)	
Data Collection	
Beamline	APS, LS-CAT-G
Wavelength (Å)	0.98
Temperature (K)	100
Space group	C 1 2 1
Cell dimension	
α, β, γ (º)	90.00, 101.15, 90.00
a, b, c (Å)	103.22, 69.78, 64.27
Resolution (Å)	50.6 (2.5)*
R_{merge} (%)	10.7 121.3)
R_{meas} (%)	12.3(141)
R_{pim} (%)	6.0 (71.1)
<I/σ>	7.6 (1.2)
CC (½)	99.3(0.59)
Completeness (%)	99.4(98.8)
Multiplicity	4.1(3.8)
No. Reflections	63914(6580)
No. Unique Reflections	15518 (1738)
Refinement	
Resolution Range	50.6 (2.5)
Number of reflections (work/test)	15472/814
R_{work} /R_{free} (%)	24.9/27.9
No. of atoms	
protein	4691
water	14
Ligand: B12	178
Cobinamide	138
B-factors(Å^2)	
Protein	57.1
Ligand: B12	67.4
Cobinamide	103.4
Water	50.0
Rmsd deviations	
Bond lengths (Å)	0.003
Bond angles (º)	0.735
Ramachandran plot (%)	
Favored, allowed, outliers	96.0, 4.0, 0
MolProbity score (percentile)	1.26(100th)
PDB code	6X8Z

*Values in parentheses are for highest-resolution shell.

Supplementary References

1. Cockle, S.; Williams, R. J. P.; Hill, H. A. O.; Ridsdale, S., Chemistry of Vitamin-B12 .16. Binding of Thiols to Cobalt(II) Corrins. *J. Chem. Soc. Dalton Trans.*1972, (3), 297-302.

2 Dimakis, N. & Bunker, G. XAFS Debye-Waller factors for Zn metalloproteins. *Phys. Rev. B* 70 (2004).